PHYSICAL REVIEW B VOLUME 43, NUMBER 6 15 FEBRUARY 1991-II

Time-resolved measurements of the radiative recombination in GaAs/$Al_xGa_{1-x}As$ heterostructures

J. P. Bergman, Q. X. Zhao, P. O. Holtz, and B. Monemar
Department of Physics and Measurement Technology, Linköping University, S-581 83 Linköping, Sweden

M. Sundaram, J. L. Merz, and A. C. Gossard
Center for Quantized Electronic Structures (QUEST), University of California, Santa Barbara, California 93106
(Received 18 May 1990)

The radiative recombination of two-dimensional (2D) carriers in an *n*-type-channel modulation-doped GaAs/$Al_xGa_{1-x}As$ heterojunction has been studied with time-resolved photoluminescence (PL). Two emission bands related to the recombination of 2D electrons, the so-called *H* band 1 (HB1) and *H* band 2 (HB2), are observed in PL. Their spectral shape and position are strongly dependent on the sample and the experimental conditions, and are, e.g., found to shift within a large photon-energy range with the excitation intensity. We have in this study measured the decay time of these PL bands as a function of recombination photon energy, under different experimental conditions. We find that the measured decay times of both the HB1 and HB2 emissions are strongly dependent on the detection photon energy. The decay times are found to increase with decreasing photon energy, in the range 1–100 ns for HB1, and 100 ns to 10 μs for HB2. This increase is explained as due to a spatial separation between the recombining electron and hole. The results are consistent with a recombination process involving 2D electrons, confined in the interface notch, and holes either from the valence band (HB1) or from neutral acceptors (HB2) in the active GaAs layer. We further show that the band bending in the active GaAs region influences the observed decay times of the HB2 emission, while the HB1 emission is almost unaffected.

INTRODUCTION

The properties of the two-dimensional (2D) electron gas formed at the interface potential in a modulation-doped GaAs/$Al_xGa_{1-x}As$ heterojunction have attracted great interest, ever since its first observation.[1] The GaAs/$Al_xGa_{1-x}As$ interface can be prepared almost free from interface defects and provides an ideal system for studying fundamental physical properties of a 2D electron gas, such as the quantized and fractional quantized Hall effect.[2,3] The high mobility of the localized 2D electrons is also of high technological interest, resulting in devices such as the high-electron-mobility transistor (HEMT).[4]

Recently, a number of photoluminescence (PL) investigations involving the 2D electrons in GaAs/$Al_xGa_{1-x}As$ heterostructures have been reported. PL emissions have been observed in samples grown by both liquid-phase epitaxy[5,6] (LPE) and molecular-beam epitaxy[7,12] (MBE) with either *n*-type or *p*-type doping in the $Al_xGa_{1-x}As$ layer, corresponding to electron or hole accumulation, respectively. The properties of the observed broad PL bands, the so-called *H* bands, vary considerably between different types of samples and different experimental conditions. One characteristic feature observed in all samples is that the PL peak position varies strongly with the optical excitation intensity, and is shifted towards higher energies with increasing excitation intensity. The observed decay times of the emissions have been reported to have values ranging from 1 ns (Ref. 7) up to 10 μs (Ref. 5).

Different recombination processes have been suggested in order to explain the observed PL properties. The most recent PL measurements of the *H* bands perturbed by a magnetic[6–10] or electric[11] field favor a model of a recombination process between quantized two-dimensional electrons confined in the interface notch and holes in the GaAs layer. A recent study has explained the drastic variation between spectra measured on different samples or at varying experimental conditions as due to different band bending on the active GaAs layer.[13]

In this paper we present detailed time-resolved measurements of the two different *H*-band emissions observed in a double heterostructure, which explain the large difference in the previously obtained decay-time results, and supports the recombination model presented in Ref. 13. Preliminary results from this work have previously been reported elsewhere.[13,14]

EXPERIMENTAL PROCEDURE

The samples used in this study were grown by MBE on a semi-insulating GaAs substrate. On top of the substrate followed a 10-period GaAs/AlAs superlattice (SL), a 500-Å-thick GaAs layer, an undoped 200-Å $Al_{0.35}Ga_{0.65}As$ spacer layer, an 800 Å n-type layer of $Al_{0.35}Ga_{0.65}As$, and finally a 50-Å-thick undoped GaAs cap layer. Both the SL and the GaAs layer were slightly *p* type ($p \approx 10^{15}$ cm^{-3}). Different samples were manufactured, in which the $Al_xGa_{1-x}As$ layer was doped with Si to a concentration of 10^{18}, 10^{17}, and 10^{16} cm^{-3}, respectively. The interface potential containing the 2D electron

 ©1991 The American Physical Society

gas is formed between the GaAs and the undoped $Al_xGa_{1-x}As$ spacer region.

The samples were placed in a combined bath and flow cryostat, and all measurements were performed at a temperature below 2 K. Both the normal PL spectral and the PL decay measurements were obtained by excitation from a cavity dumped dye laser synchronously pumped by a mode-locked Ar^+ laser. We used a DCM dye so that the laser excitation wavelength could be selected either below or above the $Al_xGa_{1-x}As$ band gap. The luminescence was dispersed through a 0.6-m-focal-length double monochromator and detected by a multi-channel-plate photomultiplier tube with $S1$ response. The PL decays were detected by a time correlated photon counting system with a time resolution better than 250 ps.

EXPERIMENTAL RESULTS AND DISCUSSION

In Fig. 1 we show a typical PL spectrum for a $GaAs/Al_xGa_{1-x}As$ n-type-channel heterostructure, obtained with pulsed excitation. The observed H-band emissions (denoted HB1 and HB2 in Fig. 1) originate from the radiative recombination between 2D electrons confined in the interface notch and holes in the GaAs layer. The excitation intensity is adjusted in such a way that the two 2D related emissions, HB1 and HB2, appear at a comparable PL intensity level. At increased excitation intensity, the high-energy band HB1 will dominate, while at lower excitation intensities only the low-energy band, HB2, can be seen. The peak positions of both HB1 and HB2 shift towards higher energies with increasing optical excitation intensity. The bound exciton (BE) and donor-acceptor-pair (DAP) recombinations are relatively stronger with the pulsed excitation compared with continuous (cw) laser excitation.[13] These BE and DAP emissions are in this case found to originate from the GaAs substrate. The increase of the PL intensity of the substrate-related emissions with pulsed excitations can be explained as saturation of the absorption in the 500-Å GaAs region, during the short (≈ 5 ps) laser excitation, increasing the penetration depth into the GaAs substrate.

The different recombination processes are further explained in Fig. 2, which schematically shows the potential for a typical heterointerface. The shape of the potential in the $Al_xGa_{1-x}As$ region is strongly influenced by the donor concentration. For the sample with highest doping, $N_D = 10^{18}$ cm^{-3}, the potential dip in the $Al_xGa_{1-x}As$ layer is expected to be deeper than with lower doping,[15] giving rise to an equilibrium electron concentration in the $Al_xGa_{1-x}As$, as well as in the active GaAs layer.

Upon optical excitation, with photon energies below the $Al_xGa_{1-x}As$ band gap, electrons and holes are created in the GaAs region. Most of these electrons are forced to the $GaAs/Al_xGa_{1-x}As$ interface notch, while the holes move towards the GaAs/SL interface, due to the built-in potential. The photoexcited holes will rapidly be captured at the ionized acceptors in the active GaAs layer, until all acceptors outside the notch region are neutral. The concentration of acceptors in the 500-Å GaAs region is about 5×10^9 cm^{-2}. The remaining free holes will form a quasiequilibrium concentration of carriers in the valence band that can recombine with the confined electrons in the conduction-band notch, resulting in the

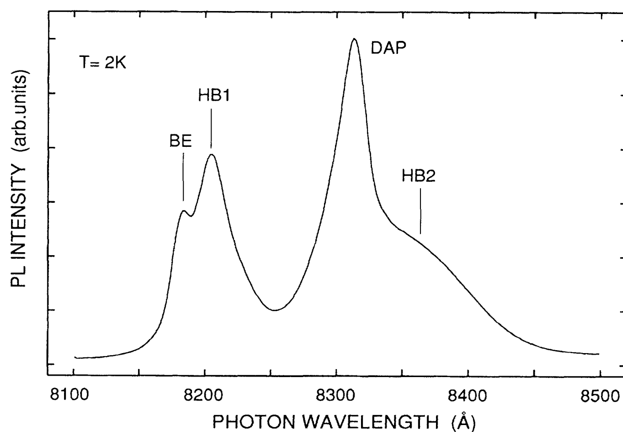

FIG. 1. Typical PL spectrum of a modulation-doped heterostructure at low temperatures, obtained with pulsed laser excitation with photon energy above the $Al_xGa_{1-x}As$ band gap. The HB1 and HB2 emissions originate from a recombination of electrons confined in the interface notch with free holes and acceptor holes, respectively. The bound exciton (BE) and the donor-acceptor-pair (DAP) recombination are believed to be related to the substrate.

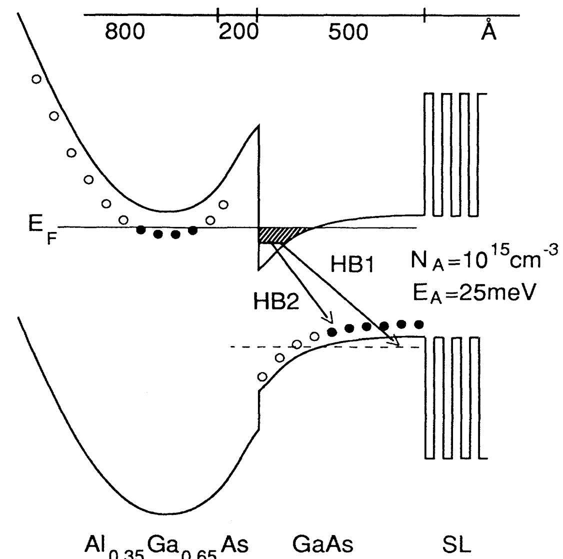

FIG. 2. A schematic drawing of the potential of a typical heterointerface. The two different recombinations, HB1 and HB2, are indicated. The dotted line in the GaAs valence band represents the effective hole quasi-Fermi-level, caused by photoexcited carriers. The relative energy between the valence and conduction bands is not drawn to scale.

HB1 PL emission.

Some care must, however, be taken during short pulsed excitation, since the intensity in the pulse is rather large, and the number of created carriers can momentarily be high. With a typical average excitation intensity of 100 mW/cm^2, a repetition frequency of 3.7 MHz, and an assumed absorption of 20% in the GaAs region, we obtain a number of initially created electron-hole pairs, for each excitation pulse, on the order of 2×10^{10} cm^{-2}. These nonequilibrium carriers affect the potential in the GaAs region in two different ways. Firstly, the total electron concentration in the interface notch increases due to the photoexcited electrons, $n_{\rm ph}$. This also increases the effective Fermi level in the notch, according to $E_{F'}=E_F+n_{\rm ph}/\rho_{\rm 2D}$ where $\rho_{\rm 2D}$ is the 2D density of states. The increase of the Fermi level is, for our case, with an excitation intensity as above, on the order of 1 meV. As a consequence of the increased electron concentration, the ground-state energy for the 2D electrons in the notch will also increase, approximately proportional to $(n_{\rm eq}+n_{\rm ph})^{2/3}$,[16] where $n_{\rm eq}$ is the equilibrium electron concentration in the notch.

Since the concentration of the photoexcited carriers decreases with time after excitation, due to electron-hole recombination, the 2D electron energy levels will change slightly during the decay measurements. This effect is expected to be small in the samples with high doping in the $Al_xGa_{1-x}As$ layer ($N_D=1\times10^{18}$ cm^{-3}), where the concentration of photoexcited electrons $n_{\rm ph}$ is much less than the equilibrium concentration $n_{\rm eq}$, estimated to be 3×10^{11} cm^{-2}. For samples with lower doping, where $n_{\rm eq}$ is smaller, the influence of the photoexcited electrons will be larger.

The photoexcited holes will also influence the potential since they neutralize the acceptors in the active GaAs region. The bending of the potential in the region outside the notch will then be reduced with increased excitation. This effect is also dependent on the time after excitation, when the acceptors are again ionized by electron-hole recombination. We believe that this influence on the electrostatic potential caused by the photoexcited holes is the major contribution to the observed energy shift of the PL emission, with increased excitation intensity.[13]

In Fig. 3 we show some typical decay curves of the HB1 emission, measured at different detection wavelengths. The curves exhibit an almost exponential decay, even if we observe an initial nonexponential part towards lower detection energies. At detection energies close to 8300 Å the recombination of the HB1 overlaps with the free to bound (FB) and DAP recombinations related to the substrate. The FB recombination is seen as the fast component in the last decay curve in Fig. 3, while the decay at even lower detection energies is totally dominated by the slow nonexponential DAP recombination from the substrate. We further observe in Fig. 3 that the decay at high photon energies is characterized by a fast decay time with a value below 1 ns, and that the decay time increases with decreasing detection photon energy. This is also seen in Fig. 4, which shows the measured decay time as a function of detection wavelength, for three samples with different doping in the $Al_xGa_{1-x}As$ region. The increase

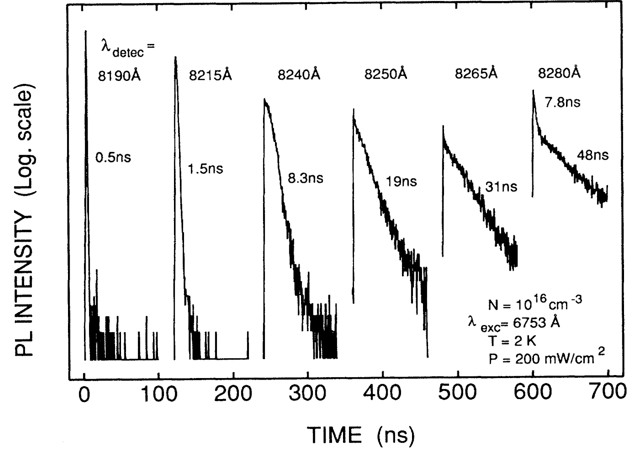

FIG. 3. Typical decay curves of the HB1 recombination measured at different spectral positions with excitation energy below the $Al_xGa_{1-x}As$ band gap. The curves are measured in the sample with lowest doping in the $Al_xGa_{1-x}As$ region, $N_D=10^{16}$ cm^{-3}. The higher background for the curves with longer decay time is due to the repetition frequency of the excitation, $f_{ML}=9.44$ MHz (corresponding to 106 ns between the pulses). For clarity, the different decay curves are shifted along the time axis.

of the observed decay time is a result of different contributing processes.

From the schematic drawing of the potential in Fig. 2 we see that the HB1 recombination occurs between spatially separated electrons and holes. The recombination probability is strongly dependent on the separation dis-

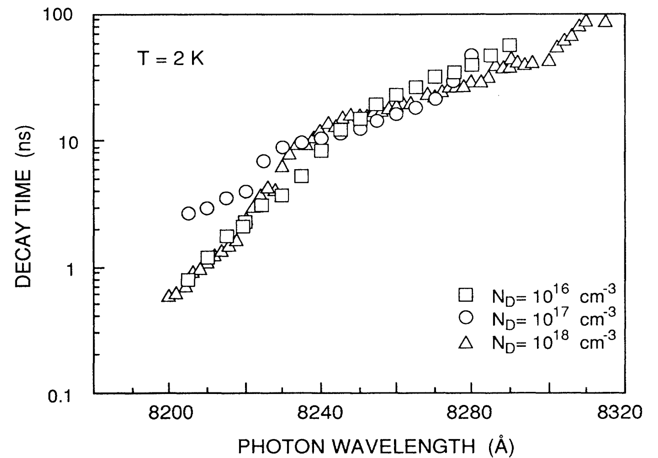

FIG. 4. The measured decay times of the HB1 recombination as a function of detection wavelength. The different curves correspond to measurements in samples with different doping in the $Al_xGa_{1-x}As$ layer. The decay times are measured with the excitation energy above the $Al_xGa_{1-x}As$ band gap with an average excitation intensity about 100 mW cm^{-2}.

tance, and the decay time can be written as

$$\tau=\tau_0 \Big/ \left| \int \varphi^e(z)\varphi^h(z) \right|^2 dz \ , \tag{1}$$

where the integral is the overlap of the electron and hole wave functions and τ_0 the decay time corresponding to maximum overlap, e.g., almost vertical transitions according to Fig. 2.[17] A larger separation, corresponding to a smaller overlap, will then give a longer decay time. Furthermore, a recombination between electrons and holes with a small separation will, due to the bending of the potential, give a higher energy compared to recombination of electrons and holes with larger separation. This explains the observed increase of the decay time with increasing detection wavelength, as seen in Fig. 4.

In addition there are other processes during pulsed excitation which influence the observed decay time. The previously discussed dynamical effects, caused by the photoexcited carriers, will shift the recombination energy from higher to lower energies, as the concentration of excess carriers decreases. The number of particles involved in the high-energy transitions will then decrease faster than expected from the radiative recombination rate. The measured decay time for these transitions is then faster than the corresponding radiative decay time as given from Eq. (1).

Such effects can also explain the partially nonexponential decay, observed for the lower recombination energies. This is seen most clearly in Fig. 3, for the curves measured with detection at 8240 Å.

The previously observed shift of the emission peak of the HB1 recombination, with decreasing excitation intensities,[13] can also be seen with pulsed excitation. In Fig. 5 we show the emission spectra measured at different time delays after the excitation pulse. The uppermost spectrum in Fig. 5 is measured during the excitation pulse, when the photoexcited carrier concentration has its maximum, and we notice that the HB1 recombination has the emission peak close to 8200 Å. With increasing time delay the peak shifts towards lower energy and disappears at about 8260 Å. We furthermore observe that the substrate-related BE emission has a very fast decay, corresponding to a decay time below 1 ns. The likewise substrate-related DAP recombination has, as expected, a longer decay time and dominates the spectra at longer time delays.

We have also measured the decay of the HB2 recombination, which is interpreted as the recombination of the 2D electrons confined in the GaAs/$Al_xGa_{1-x}As$ interface potential, with holes bound at acceptors in the active GaAs region. These measurements are made with a low excitation intensity ($\approx 10 mW/cm^{-2}$), and it is usually not possible to observe the HB1 recombination under these conditions. The previously discussed effects, caused by an increase of the electron concentration in the notch, can in this case be neglected. The potential in the 500-Å GaAs layer will, however, change during the decay measurement, due to the change in charge state of the acceptor, when the hole bound at the acceptor recombines. The importance of this is difficult to estimate without a detailed knowledge of the band potentials.

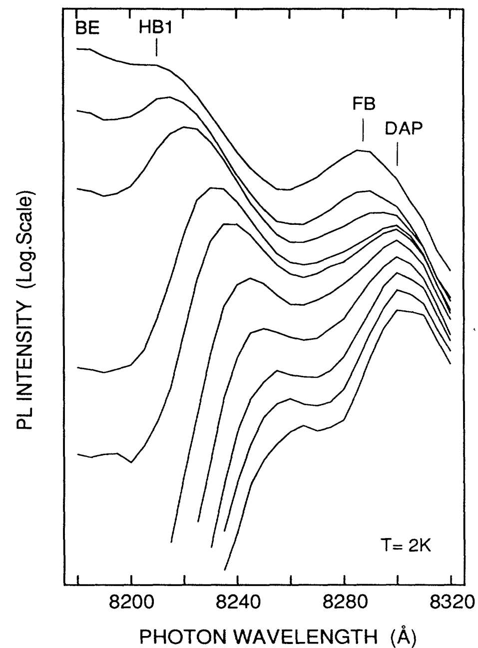

FIG. 5. PL spectra of the HB1 recombination measured at different time delays after the excitation pulse. The measurements are done with high excitation intensity and an excitation energy above the $Al_xGa_{1-x}As$ band gap, in a sample with $N_D=10^{18}$ cm^{-3}. The time delay is, from top to bottom, 0, 1.2, 2.4, 4.8, 9.6, 20, 32, 55, 78, and 100 ns. Note the logarithmic scale for the PL intensity.

Typical decay curves for the HB2 recombination, with low intensity excitation below the $Al_xGa_{1-x}As$ band gap, are shown in Fig. 6. The curves exhibit a single exponential decay, as is expected for a recombination between holes bound at an acceptor with 2D electrons localized in the notch. In contrast to the case of the HB1 recombination, we observe significant differences in the decay time of the HB2 recombination measured in different samples. This can be seen in Fig. 7, which shows the measured decay time as a function of detection wavelength, for samples with different doping in the $Al_xGa_{1-x}As$ layer. One possible explanation for this can be that a higher doping in the $Al_xGa_{1-x}As$ causes an increased bending of the band potential in the GaAs region outside the interface notch, due to the higher electron concentration in the notch. With a larger bending, the variation of the recombination energy as a function of distance from the interface will be larger. The increase of the decay time will then occur over a wider energy range, as can be seen in Fig. 7 for the highly doped sample, $N_D=10^{18}$ cm^{-3}. The higher electron concentration in the notch, giving electrons with a large energy distribution E_F-E_0, will also contribute to the large variation in observed recombination energies.

Following the arguments given above, we expect a sample with lower doping, N_D, to have more flat band

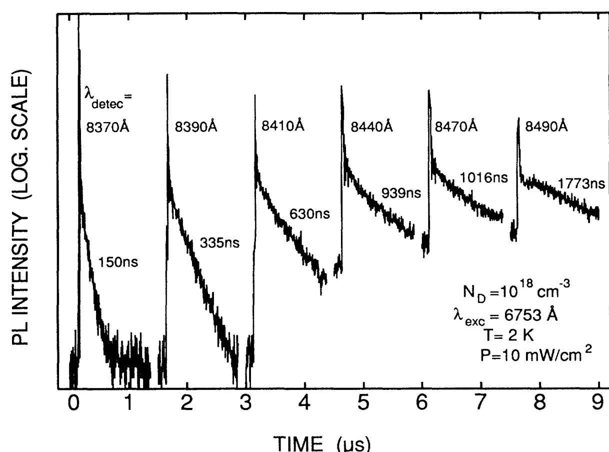

FIG. 6. Decay curves of the HB2 recombination measured at different detection wavelengths, obtained with excitation below the $Al_xGa_{1-x}As$ band gap. The increased background level for the last curves, which has a relatively longer decay time, is due to an overlap with the decay from the preceding laser pulse.

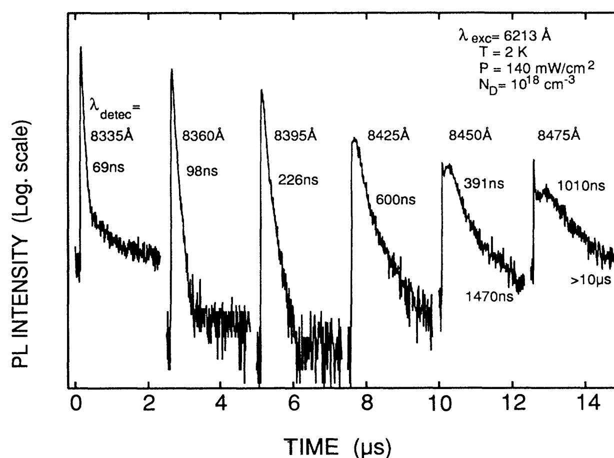

FIG. 8. Decay curves measured at different detection wavelengths, with excitation above the $Al_xGa_{1-x}As$ band gap. The slow component in the first curve is due to overlap with the DAP emission. The values corresponding to the exponential decay time are also shown.

potential in the region where the acceptors involved in the HB2 recombination are located. The energy difference between different recombinations will then be smaller than in the high doping case. We will consequently observe a large increase of the decay time, in a relatively narrow recombination energy range. This is seen in Fig. 7, represented by the sample with lowest doping, $N_D = 10^{16}$ cm^{-3}.

The values of the observed decay time for the HB2 recombination are longer than for the HB1 recombination, and are at low energies longer than the upper time resolution of our detection system (≈ 10 μs). In some measurements we observe an initial very fast decay, whose origin is not fully understood.

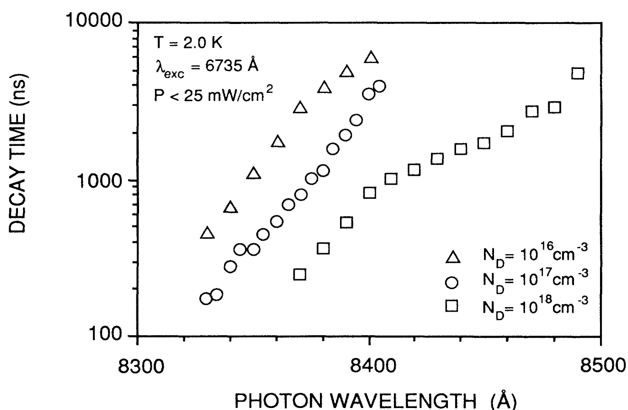

FIG. 7. The observed decay time of the HB2 recombination measured as a function of the detection wavelength. The different curves correspond to samples with different n-type doping in the $Al_xGa_{1-x}As$ layer.

The measured decay time at a fixed detection energy of both the HB1 and HB2 recombination is independent of the excitation intensity, if the excitation is below the $Al_xGa_{1-x}As$ band gap. With above-band-gap excitation, some changes occur together with an increased nonexponentiality of the observed decay. We believe that this is mainly due to changes in the band bending caused by the high concentration of nonequilibrium carriers. Figure 8 shows typical decay curves of the HB2 recombination measured at different wavelength positions, with above-band-gap excitation. The HB2 is shifted towards higher energies, as compared to the case with below-band-gap excitation. In the lower-energy decay curves in Fig. 8, we observe a saturation of the decay at short times after excitation. This is, as discussed before, due to trapping of photoexcited holes to neutral acceptors. The concentration of neutral acceptors will be constant as long as free holes exist in the valence band, and the decay will ideally have a flat initial part. The time during which this saturation can be observed, is comparable to the measured decay time of the corresponding HB1 recombination.

It should finally be noted that we observe no PL emissions that are possible to relate to excited energy levels in the interface notch. One possible explanation for this can be that since such an emission is expected to have a decay time and recombination energy similar to that of the substrate-related BE emission, it will not be possible to experimentally distinguish these two emissions.

SUMMARY

We have in this study presented time decay measurements of two PL emission bands, HB1 and HB2, related to 2D electrons in a modulation-doped $GaAs/Al_xGa_{1-x}As$ heterointerface. Our results are con-

sistent with the proposed models for the two emissions, where the 2D electrons recombine with holes in the valence band (HB1) and holes bound at acceptors in the active GaAs region (HB2), respectively. The increase of the observed decay time of the HB1 and HB2 emissions, at lower photon energies, is quantitatively explained by a tunneling process between spatially separated particles. Theoretical calculations to verify our experimental results, which includes detailed calculation of the band potential, are underway.

ACKNOWLEDGMENTS

This work was partially supported by the NSF Science and Technology Center for Quantized Electronic Structure (QUEST).

[1] H. L. Störmer, R. Dingle, A. C. Gossard, W. Wiegmann, and M. D. Sturge, Solid State Commun. **29**, 705 (1979).

[2] K. V. Klitzing, G. Dorda, and M. Pepper, Phys. Rev. Lett. **45**, 494 (1980).

[3] H. L. Störmer, A. Chang, D. C. Tsui, J. C. M. Hwang, A. C. Gossard, and W. Wiegmann, Phys. Rev. Lett. **50**, 1953 (1993).

[4] See, e.g., H. Morkoç and H. Unlu, in *Applications of Multiquantum Wells, Selective Doping, and Superlattices* (unpublished); in *Semiconductors and Semimetals,* edited by R. K. Willardson and A. C. Beer (Academic, London, 1987), Vol. 24.

[5] Y. R. Yuan, M. A. A. Pudensi, G. A. Vawter, and J. L. Merz, J. Appl. Phys. **58**, 397 (1985).

[6] Y. R. Yuan, K. Mohammed, M. A. A. Pudensi, and J. Merz, Appl. Phys. lett. **45**, 739 (1984).

[7] Zh.I. Alferov, A. M. Vasil'ev, P. S. Kop'ev, V. P. Kochereskho, I. N. Ural'tsev, Al.L. Efros, and D. R. Yakovlev, Pis'ma Zh. Eksp. Teor. Fiz. **43**, 442 (1986) [JETP Lett. **43**, 569 (1986)].

[8] H. L. Störmer, R. Dingle, A. C. Gossard, W. Wiegmann, and M. D. Sturge, Solid State Commun. **29**, 705 (1979).

[9] W. Ossau, E. Bangert, and G. Weimann, Solid State Commun. **64**, 711 (1987).

[10] I. V. Kukushkin, K. von Klitzing, and K. Ploog, Phys. Rev. B **37**, 8509 (1988).

[11] I. V. Kukushkin, K. von Klitzing, K. Ploog, V. E. Kirpichev, and B. N. Shepel, Phys. Rev. B **40**, 4179 (1989).

[12] I. V. Kukushkin, K. von Klitzing, K. Ploog, and V. B. Timofeev, Phys. Rev. B **40**, 7788 (1989).

[13] Q. X. Zhao, J. P. Bergman, P. O. Holtz, B. Monemar, M. Sundaram, J. L. Merz, and A. C. Gossard, Semicond. Sci. Technol. **5**, 884 (1990).

[14] J. P. Bergman, Q. X. Zhao, P. O. Holtz, B. Monemar, M. Sundaram, J. L. Merz, and A. C. Gossard, in Proceedings MRS fall meeting, Boston 1989.

[15] N. T. Thang, G. Fishman, and B. Vinter, J. Appl. Phys. **59**, 499 (1986).

[16] C. Weisbuch, in *Applications of Multiquantum Wells, Selective Doping, and Superlattices,* edited by R. Dingle (unpublished); in *Semiconductors and Semimetals,* edited by R. K. Willardson and A. C. Beer (Academic, London, 1987), Vol. 24.

[17] K. Köhler, H.-J. Polland, L. Schultheis, and C. W. Tu, Phys. Rev. B **38**, 5496 (1988).